Coupling Model of Fuzzy Soft Set and Bayesian Method to Forecast Internal Defects of Ancient Wooden Structures Based on Nondestructive Test

Ziyi Wang,[a,c,d] Wei Wang,[b,c,d,*] Donghui Ma,[b,c,d] Xiaodong Guo,[b,c,d] Junhong Huan,[a,c,d] and Liting Cheng [a]

In order to improve the detection precision of internal defect in the ancient wooden structures, defect simulation tests on pine and elm commonly used in ancient buildings were performed by using stress wave detection and drilling resistance detection. Based on detection data, three typical evaluation criteria, which are the information entropy, the correlation coefficient, and residual sum of squares, were selected as a priori information. Combining with the expert's fuzzy evaluation value, Bayesian formula was used to modify the prior information to determine the weight coefficients of the two detection methods, and a combined prediction model was established. The results show that the combination of subjectivity and objectivity enables the revised weights to more reasonably and accurately reflect the relative importance of each detection method in prediction evaluation, which reduces the forecasting error. Specifically speaking, the mean error of the combined model was reduced by 49.8% and 59.8%, respectively, compared with stress wave detection and drilling resistance detection. Moreover, the five error indicators of this combined forecasting model are the smallest in all methods, indicating the proposed method has a better forecasting effect. It provides an effective application tool for the practice of forecasting the internal defects of wooden components in ancient buildings.

Keywords: Ancient building; Wooden structure; Internal defect; Non-destructive tests; Combined forecasting model; Fuzzy soft set; Bayesian method

*Contact information: a: College of Architecture and Civil Engineering, Beijing University of Technology, Beijing 100124, China; b: College of Architecture and Urban Planning, Beijing University of Technology, Beijing 100124, China; c: Institute of Earthquake Resistance and Disaster Reduction, Beijing University of Technology, Beijing 100124, China; d: Key Science Research Base of Safety Assessment and Disaster Mitigation for Traditional Timber Structure (Beijing University of Technology), State Administration for Cultural Heritage, Beijing 100124, China; *Corresponding author: ieeww@bjut.edu.cn*

INTRODUCTION

Compared with the masonry structure system of western ancient architecture, the most important feature of Chinese ancient architecture is that the building adopts a wooden structure system (Kim and Park 2017). However, timber components in ancient buildings often appear decayed, with insect attacks and hollow spaces (Fig. 1) after several hundred years or even thousands of years (Gao *et al.* 2018; Broda and Popescu 2019). As a result, the physical and mechanical properties are attenuated, which ultimately leads to the damage and the reduction of mechanical strength of wooden structure in ancient buildings (Calderoni *et al*. 2010; Qin and Yang 2016). For example, the Qinzhuang Dongyue Temple (Fig. 2a), the Jade Emperor Temple (Fig. 2b), and the Puming Temple (Fig. 2c), built in the Yuan Dynasty, are historical buildings in Shanxi Province, China. The Xia Jin Confucian Temple (Fig. 2d), built in the Song Dynasty, is a historical building in Shandong

Province, China. Due to the lack of maintenance, long cracks, hollows, and insects appeared in the beams or columns, which eventually cause the roof to collapse.

The protection of wooden structures that have been used for hundreds of years has become a top priority in the maintenance and repair of ancient buildings in China. To ensure that the authenticity of the ancient structure is not destroyed and to accurately assess the health status of the wooden structure, it is necessary to obtain the internal damage information of wooden structures in the ancient buildings by nondestructive testing (Chen and Guo 2017; Voessing and Niederleithinger 2018).

Fig. 1. Damaged characteristics of (a) decay, (b) hollow, (c) insect attacks, (d) crack

Fig. 2. Destruction of wooden structures in (a) Dongyue Temple, (b) Jade Emperor Temple, (c) Puming Temple, (d) Xia Jin Confucian Temple

Many non-destructive testing methods have been developed, such as ultrasonic detection (Gatto *et al*. 2012; Vossing *et al*. 2018; Espinosa *et al*. 2019), X-ray detection (Pease *et al*. 2012; Franke *et al*. 2013; Riggio *et al*. 2015), pin impact tests (Huang *et al*. 2010; Wu *et al*. 2010), stress wave detection (Rust and Göcke 2000; Dackermann *et al*. 2014; Li *et al*. 2015), and drilling resistance detection (Isik and Li 2003; Kasal and Anthony 2004; Nowak *et al*. 2016). Pin impact tests, stress wave detection, and drilling resistance detection are the more common methods (An *et al*. 2008), but it is difficult to carry out a comprehensive and accurate assessment of the internal damage of wooden structures using only one method. To make up for the shortcomings of each method, different detection methods have been combined to analyze quantitatively and qualitatively the internal damage of wood (An *et al*. 2008; Ge *et al*. 2014; Wang and Allison 2008; Ouis and Zerizer 2006; Choi *et al*. 2007). Moreover, there are already several publications reporting on the determination of weights related to the combination of different nondestructive tests (Chang *et al*. 2016a,b; Dai *et al*. 2017; Chang *et al*. 2019; Wang *et al*. 2019). However, these combined forecasting models are often built solely based on specific evaluation criteria, and they only consider objective test data and ignore experts' experience when determining the weights of the combined model. Therefore, the forecasting effect often has a large error relative to the actual situation. In fact, there are often large differences between the results of different detection methods. In the process of actual detection, experts often need to conduct field investigation based on experience, so as to subjectively and

objectively give the forecasting results consistent with the actual situation. Based on the detection data and expert experience, one attempts to determine the weights of the combined model by using the experts' evaluation fuzzy value to correct the prior information of nondestructive test, hoping to improve the precision of forecasting internal defects of wooden members.

Combined Forecasting Model of Internal Defect of Timber Components

When the stress wave detection method and drilling resistance detection method are used alone, their detection precision is usually relatively low, and it is difficult to obtain more comprehensive information on internal defects of wooden members (Wang *et al.* 2019). To be more specific, the detected image obtained by the stress wave detection method can intuitively show the decay distribution of the measured section, but the boundary of the image is very fuzzy and the detection results are not accurate enough. Meanwhile, the drilling resistance detection method can accurately reflect the material condition along the test direction, and it often requires multiple paths for detection, which will cause damage to the ancient wooden structure (Chang *et al.* 2016b; Wang *et al.* 2019). Therefore, a combined forecasting model is established in this work based on the stress wave detection and drilling resistance detection according to the characteristics of internal damage in wooden structure. Combined forecasting method can set up the coordination model based on a single detection method by combining the weight coefficients, which can achieve better forecasting effect. It is generally known that determining the combined weight coefficients is essential for combined forecasting method (Huang *et al.* 2015; Zhou and Wang 2009). At present, there are three types of methods, as follows:

(1) According to evaluation criterion of a certain detection result, the optimization model is constructed to obtain the combined weighting coefficients (Chen and Hou 2003). However, this method is one-sided, and the forecasting effect evaluation indexes are various, which cannot improve forecasting effects.

(2) The weight coefficients of the criterion are determined by using multi-criteria decision method, such as the entropy method. However, when the weight coefficients are determined by the entropy method, there is no guarantee that the combined forecasting value is better than the single method (Zhu and Yan 2004).

(3) The information aggregation operator is used to determine the combined weight coefficients (Aggarwal 2015; Chen and Sheng 2005). This method relies on the knowledge background of each decision maker and has strong subjectivity.

In view of the above situations, according to the diversity of forecasting effect evaluation criteria, this paper selected three typical evaluation criteria—the information entropy (Shannon 1948; Lianxiao and Morimoto 2019), the correlation coefficient, and the residual sum of squares—to be *a priori* information. Combined weight coefficients of two detection methods are determined by using the unrestricted advantages of fuzzy soft set parameter tools and the advantage of Bayesian formula in modifying prior information (Sun 2014; Dong *et al*. 2018). The combination of subjectivity and objectivity can reduce the forecasting error, which provides an effective method for forecasting the internal damage of ancient wooden structures. The combined forecasting model of internal damage in wood under the condition t is as follows:

$$\hat{S}_t = l_1^* S_{1t} + l_2^* S_{2t} \quad t = 1,2,\cdots,20 \tag{1}$$

where l^*_1 represents the corrected weight of stress wave detection value (S_{1t}), l^*_2 represents the corrected weight of drilling resistance detection value (S_{2t}), $l^*_1+l^*_2=1$.

Combinatorial Coefficients Based on Fuzzy Soft Set and Bayesian Method

Determine evaluation criteria

The detection error value refers to the difference between the actual value and the detection value. The smaller the error value is, the higher the precision of the detection result is. In order to measure the quality of a detection method, it is necessary to analyze the detection error within the original working condition. In this paper, the information entropy, the correlation coefficient and the residual sum of squares are selected as the evaluation criteria of detection error.

(1) Information entropy

Information entropy is a quantity that represents the overall information measure of information sources. For a particular information source, the information entropy is a certain value. Information entropy represents the average uncertainty and randomness of the system, which is a measure of the disorder degree of the system. If a system is random and disorderly, its information entropy must be large. If the system has certain rules, then the information entropy is small (Shannon 1948).

In 1948, Shannon abstracted mathematics of information entropy as the uncertainty degree of the sample space within which the probability is P_t under working condition (X_t). In the probabilistic system, there are n working conditions (X_1, X_2, …, X_n). When working condition (X_t) occurs, the information content is H_t=-$P_t lnP_t$. For the probabilistic system with n working conditions, the average information content is denoted as $H(P_1, \ldots, P_n)$ that is defined as follows,

$$H(P_1,\cdots,P_n)=\sum_{t=1}^{n}H_t=-\sum_{t=1}^{n}P_t\ln P_t \tag{2}$$

where, $\sum_{t=1}^{n}p_t=1$.

$$e_i(t)=\begin{cases}1 & \dfrac{|S_t-S_{it}|}{S_t}\geq 1\\ \dfrac{|S_t-S_{it}|}{S_t} & 0\leq\dfrac{|S_t-S_{it}|}{S_t}<1\end{cases} \tag{3}$$

where $e_i(t)$ is the relative error of the i-th detection method in the condition t, and $\{e_i(t); i=1, 2, t=1,2,...,20\}$ is the relative error sequence of the i-th detection method under working condition t.

The relative error sequences of each detection methods are normalized to calculate the proportion of the relative error of the i-th detection method in the working condition t.

$$p_i(t)=\frac{e_i(t)}{\sum_{t=1}^{n}e_i(t)} \tag{4}$$

$$\sum_{t=1}^{n}p_i(t)=1 \tag{5}$$

The entropy value of the relative error of the i-th detection method is calculated as follows,

$$h_i=-k\sum_{t=1}^{n}p_i(t)\ln p_i(t) \tag{6}$$

where k (k>0) is a constant. For the i-th detection method, if $p_i(t)$ are all equal ($p_i(t)$=1/n), h_i is going to be the maximum (h_i=$k$ln$n$), where k is taken 1/ln$n$, so there is 0≤h≤1.

From the definition of information entropy, it can be concluded that the smaller the entropy of a detection error sequence of a single detection method is, the greater its variation is (Lianxiao and Morimoto 2019).

(2) Correlation coefficient

In multivariate analysis, the correlation coefficient is an indicator to measure the direction and degree of linear correlation between two random variables. The closer the detection value is to the actual value, the higher the correlation degree of the two sequences is. Therefore, correlation coefficient can be used to measure the detection precision. In this paper, the correlation coefficient (r_i) between the detection sequence (S_{it}) and the actual sequence (S_t) is typically expressed as follows:

$$r_i = \frac{\sum_{t=1}^{n} \left| S_{it} - \bar{S}_i \right\| S_t - \bar{S}_t \right|}{\sqrt{\sum_{t=1}^{n} \left(S_{it} - \bar{S}_i \right)^2} \sqrt{\sum_{t=1}^{n} \left(S_t - \bar{S}_t \right)^2}} \quad (7)$$

Where, $\bar{S}_i = \frac{1}{n}\sum_{t=1}^{n} S_{it}, \bar{S}_t = \frac{1}{n}\sum_{t=1}^{n} S_t$.

(3) Residual sum of squares

In order to clearly explain what is the effect of each variate and random error. In statistics, the residual is the difference between the data point and its corresponding position on the regression line. The residual sum of squares represents the effect of random errors. The smaller the residual sum of squares is, the better the fitting degree is. In this paper, the square error sum (Q_i) is taken as an indicator to reflect the detection precision, Q_i can be defined as follows:

$$Q_i = \sum_{t=1}^{n} e_{it}^2 = \sum_{t=1}^{n} \left(S_t - S_{it} \right)^2 \quad (8)$$

Theory of fuzzy soft set and Bayesian formula

Molodtsov (1999) proposed the soft set theory. At present, soft set theory has become a general mathematical tool for dealing with uncertain and fuzzy objects. It is often used in decision-making, evaluation, parameter reduction, index weight determination, soft algebra, and prediction (Kovkov *et al*. 2007; Yue *et al*. 2013).

Definition 1 (soft set): Suppose that U is the initial discourse domain and L is the parameter set, $P(U)$ is the power set of U, (F, L) is a soft set of U, if and only if F is a mapping from L to $P(U)$. Each $F(l)$ ($l \in L$) can be regarded as the set of l-elements in the soft set (F, L).

Definition 2 (fuzzy soft set): Suppose that U is the initial discourse domain and L is the parameter set, $\varepsilon(U)$ is the fuzzy set defined on U. (F, A) ($A \subseteq L$) is a fuzzy soft set on the discourse domain U, if and only if F is a mapping from A to $\varepsilon(U)$.

Definition 3 (Bayesian formula): Suppose that S is the sample space of test E, and A is the event of E, $(B_1, B_2, \ldots, B_n)$ is a division of S, and $P(A)>0$, $P(B_i)>0$ ($i=1,2,\ldots,n$), then the Bayesian formula can be expressed as follows:

$$P\left(B_i \middle| A\right) = \frac{P\left(A \middle| B_i\right) P\left(B_i\right)}{\sum_{j=1}^{n} P\left(A \middle| B_j\right) P\left(B_j\right)} \quad (9)$$

To sum up, the steps to determine the combined weight coefficients based on fuzzy

soft set and Bayesian method are as follows:

Step1: According to the detection results, the evaluation criteria (information entropy, correlation coefficient and residual sum of squares) for the detection results of two detection methods are calculated. Delphi method is used to perform fuzzy evaluation on the parameters of the evaluation criteria, and the fuzzy soft set (F, A) is input.

Step2: Input the initial discourse domain U.

Step3: Combining with the weights given by experts, the Bayesian formula (Eq.9) is used to modify the weights determined by the three evaluation criteria, respectively.

Step4: Calculate the average of the corrected weights.

EXPERIMENTAL

Non-Destructive Tests

Test Materials

Pine and elm, commonly used in the ancient wooden structures, were selected as test specimens. Through visual inspection, surface percussion, and pressing, there were no obvious joints, splits, or other damage on specimens. The test specimens were processed into round test pieces (Chang *et al.* 2016a; Wang *et al.* 2019). Table 1 shows the specific parameters. The average moisture content of the four specimens met the requirements of the GB/T 50005 (2017) and GB/T 50329 (2012) standards. Then, five standard circles are drawn on each specimen.

Table 1. Test Specimen Number and Parameters

Working Conditions	Damaged Proportion	Simulation Type	Tree Species	Radius (mm)	Moisture Content (%)	Detected Height (mm)
1	1/9	Hollow	Pine (Specimen 1)	154	14.2	50
2	1/7					
3	1/5					
4	1/3					
5	1/2					
6	1/9	Hollow	Elm (Specimen 2)	175	10.7	50
7	1/7					
8	1/5					
9	1/3					
10	1/2					
11	1/9	Insect attacks	Pine (Specimen 3)	145	12.5	50
12	1/7					
13	1/5					
14	1/3					
15	1/2					
16	1/9	Insect attacks	Elm (Specimen 4)	178	10.9	50
17	1/7					
18	1/5					
19	1/3					
20	1/2					

The area of these five circular areas represented 1/9, 1/7, 1/5, 1/3 and 1/2 of the cross section area of each specimen, respectively (Fig. 3a). According to the idea of reverse

simulation, the internal hollow and insect attacks were simulated by manual digging (Fig. 3b) and drilling (Fig. 3c) in the specimens. In addition, the diameter of the drilling is about 10 mm, and the distance between the drilling is about 5mm (Fig. 3c).

(a) Damaged proportion **(b)** Manual digging **(c)** Manual drilling

Fig. 3. Making test specimens

Test conditions

The indoor temperature was 20 °C with 72% relative humidity. The test equipment (Fig. 4) was stress wave testing instrument (Fakopp, Enterprise, Hungary), drilling resistance testing instrument (IML-PD500, IML Co., Ltd., Wiesloch, Germany), wood moisture meter (GANN-HT85T, Gann Mess-u. Regeltechnik GmbH, Germany) and electric percussion drill (GSR18-2-LI, Robert Bosch GmbH, Stuttgart, Germany).

(a) **(b)** **(c)** **(d)**

Fig. 4. (a) Fakopp, (b) IML-PD500, (c) GANN-HT85T, (d) GSR18-2-LI

Stress Wave Detection

The Fakopp 3D acoustic tomograph (Fig. 5 and Fig. 6) is able to non-destructively detect the size and location of decayed or hollow parts in the trunk. It works based on sound velocity measurement between several sensors around the trunk. If there is a hole, the sound waves have to pass around the hole, and it requires more time to reach the opposite sensors. In order to explain the complex velocity model, a two-dimensional image is constructed. Healthy wood is shown in green, decaying wood is shown in red, and hollow is shown in blue. This test selects 10 sensors to detect the internal damage of the specimen. The damaged area (S_{1t}) can be calculated according to detected damaged percentage which is obtained by stress wave ArborSonic 3D software.

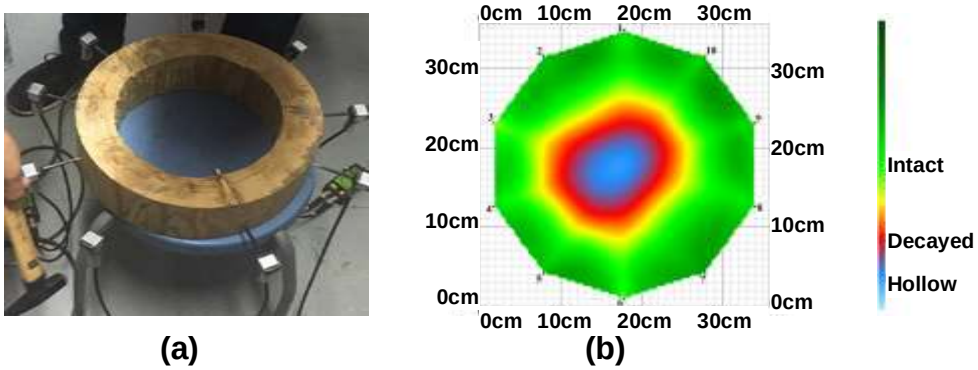

Fig. 5. Stress wave detection for (a) hollow, (b) two-dimensional image of hollow

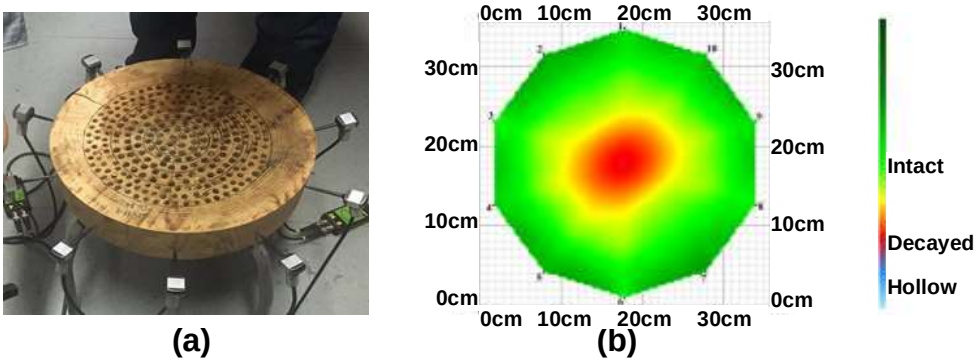

Fig. 6. Stress wave detection for (a) Insect attacks, (b) two-dimensional image of Insect attacks

Drilling Resistance Detection

The IML-PD500 instrument (Fig. 7 and Fig. 8) uses a small needle, driven by a motor, to penetrate into the wood at a constant speed. The impedance curve is displayed on the display screen of the instrument. Drilling resistance detection is used to detect and judge the decay, hollow, and insect attacks of the wood. It can be used for the detection and evaluation of all trees and wooden structures. Because drilling resistance detection can only detect the damage of the wood in a single path, the test selects three paths to detect the specimen. The length of the internal damage measured for each path is d_1, d_2 and d_3. The damaged area (S_{2t}) can be calculated by Eq. 10 (Chang *et al*. 2016a).

$$S_{2t} = \frac{1}{2} \times d_1 \times d_2 \times d_3 \times \sin\frac{360^\circ}{n} \quad (10)$$

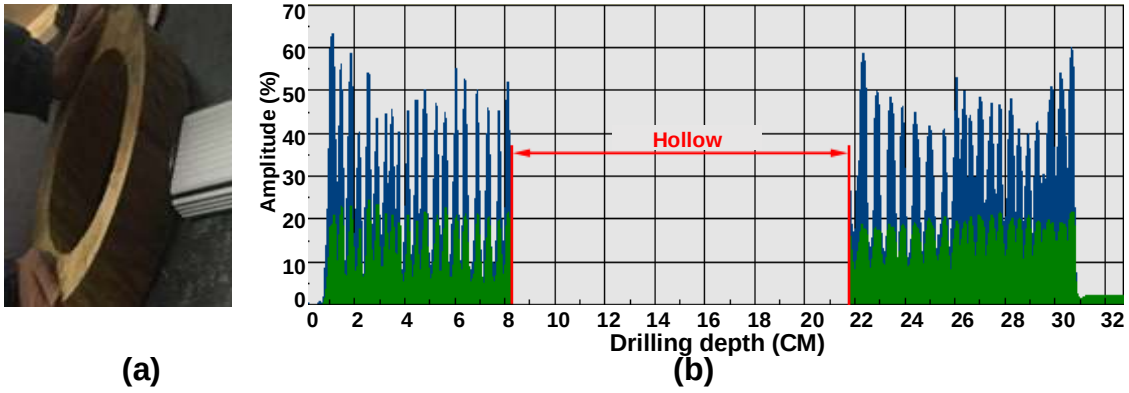

Fig. 7. Drilling resistance detection for (a) hollow, (b) two-dimensional image of hollow

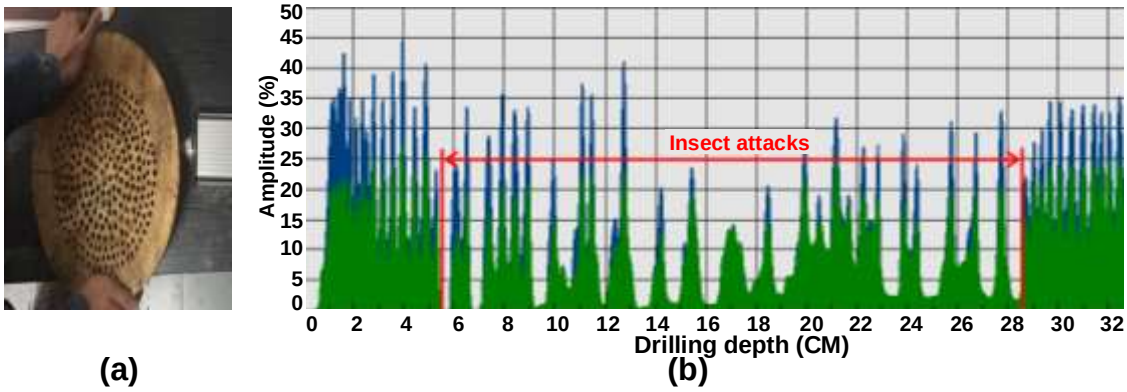

Fig. 8. Drilling resistance detection for (a) Insect attacks, (b) two-dimensional image of Insect attacks

RESULTS AND DISCUSSION

Two-dimensional Images

Taking the specimen 2 with a damaged proportion of 1/5 as an example, it simulated the damage condition of a hollow elm piece. Figure 9 shows the two-dimensional image obtained by two detection methods. The damage type represented by the bright blue area in the stress wave detection image is hollow, which damaged percentage obtained by stress wave ArborSonic 3D software is approximately 13%. It can be seen from Fig. 9b that the size and position of this bright blue area is close to the actual damaged area, but the boundary of this bright blue area is blurred. After this specimen was tested by multiple paths through the drilling resistance detection, it is found that the two-dimensional image obtained by the drilling resistance detection shows only the width of the internal damage of the wood in a single path and could not display the image of the overall damage in wood (Fig. 9c). Meanwhile, after comparing the two-dimensional images measured by two detection methods under different damage proportion, we found that as the internal damaged proportion of the specimen increases, the bright blue area in the two-dimensional image obtained by the stress wave detection and the "blank" part of the image detected by the drilling resistance detection also increases, which are similar to the test results mentioned in the reference (Chang *et al*. 2016a; Wang *et al*. 2019).

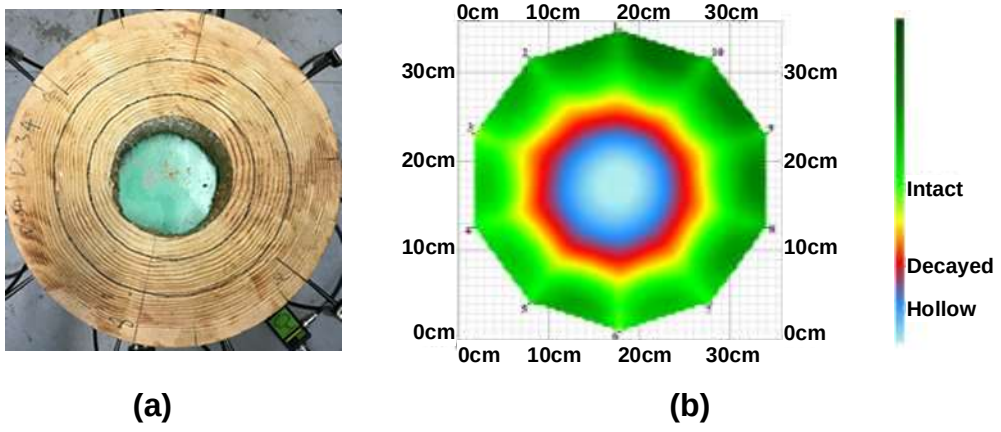

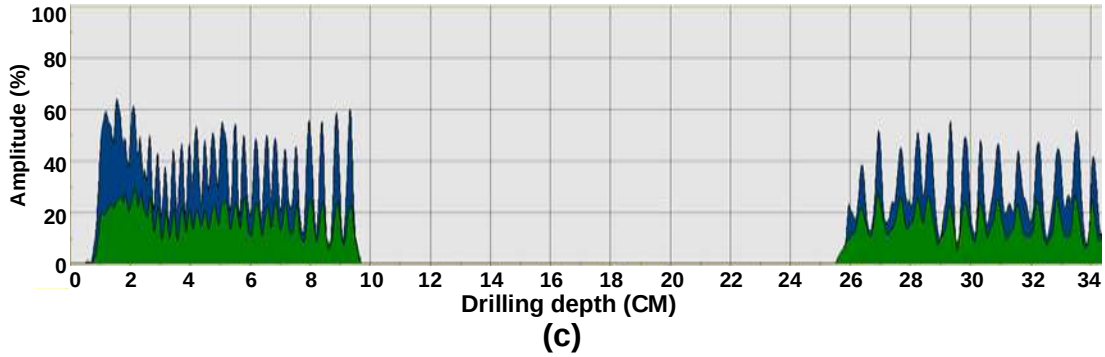

Fig. 9. (a) Specimen 2 with a damaged proportion of 1/5, (b) two-dimensional image obtained by the stress wave detection, (c) two-dimensional image obtained by the drilling resistance detection

Detection Data

Taking the detection data in the paper (Chang *et al*. 2016a) as an example, the results listed in Table 2 show the detection precision p_{it} of each method under 20 working conditions, where $p_{it}=\frac{|S_t-S_{it}|}{S_t}\times 100\%, i=1,2. t=1,2,...,20.$ It is obvious that the detection precision of the same detection method under different working conditions was different, and the detection precision of different detection methods under the same working condition was also different. Meanwhile, Table 2 also shows the mean absolute error *AVG* (e_i) of each method under 20 working conditions, where $AVG(e_i)=\sum_{t=1}^{20} e_{it}=|S_t-S_{it}|, i=1,2. t=1,2,...,20$ (Chang *et al*. 2016a). The average absolute errors of the stress wave detection and drilling resistance detection were 22.06 cm^2 and 27.53 cm^2, respectively, indicating that the overall effect of stress wave detection was slightly better than that of drilling resistance detection. However, the overall error of the stress wave detection method and drilling resistance detection method was very large, and their precision needed to be further improved.

Table 2. Results and Accuracy of the Two Detection Methods

Working conditions	Damaged proportion	Simulation type	Tree species	S_t	M-1			M-2		
					S_{1t}	e_{1t}	p_{1t}	S_{2t}	e_{2t}	p_{2t}
1	1/9	Hollow	Pine (Specimen 1)	83.28	122.43	39.15	52.99%	51.53	31.75	61.88%
2	1/7			107.07	127.41	20.34	81.00%	88.76	18.31	82.90%
3	1/5			149.90	164.89	14.99	90.00%	113.97	35.93	76.03%
4	1/3			249.84	262.33	12.49	95.00%	215.09	34.75	86.09%
5	1/2			374.76	392.78	18.02	95.19%	337.64	37.12	90.09%
6	1/9	Hollow	Elm (Specimen 2)	73.76	83.02	9.26	87.45%	67.74	6.02	91.84%
7	1/7			94.83	115.99	21.16	77.69%	73.24	21.59	77.23%
8	1/5			132.77	129.68	3.09	97.67%	116.68	16.09	87.88%
9	1/3			221.28	248.49	27.21	87.70%	199.50	21.78	90.16%
10	1/2			331.92	352.75	20.83	93.72%	304.81	27.11	91.83%
11	1/9	Insect attacks	Pine (Specimen 3)	107.09	154.21	47.12	56.00%	77.68	29.41	72.54%
12	1/7			137.69	173.49	35.8	74.00%	104.99	32.70	76.25%
13	1/5			192.76	221.68	28.92	85.00%	144.82	47.94	75.13%
14	1/3			321.27	342.34	21.07	93.44%	280.38	40.89	87.27%

15	1/2			481.91	462.63	19.28	96.00%	420.31	61.60	87.22%
16	1/9	Insect attacks	Elm (Specimen 4)	112.61	128.04	15.43	86.30%	104.18	8.430	92.51%
17	1/7			144.21	131.23	12.98	91.00%	129.20	15.01	89.59%
18	1/5			201.89	211.98	10.09	95.00%	185.47	16.42	91.87%
19	1/3			336.48	312.93	23.55	93.00%	313.62	22.86	93.21%
20	1/2			504.73	464.38	40.35	92.01%	479.78	24.95	95.06%
Mean value						22.06			27.53	

Note: S_t is the actual value under each working condition (unit: cm^2); S_{1t} and S_{2t} are the detection value of stress wave detection and drilling resistance detection, respectively (unit: cm^2); e_{1t} and e_{2t} are the absolute error of stress wave detection and drilling resistance detection, respectively (unit: cm^2); p_{1t} and p_{2t} are the precision of stress wave detection and drilling resistance detection under each working condition. M-1 and M-2 represents the stress wave detection method and the drilling resistance detection method, respectively.

For pine, Figs. 10a and 10c show that the precision of stress wave detection increased with the increasing damaged proportion. When the damaged proportion exceeded 1/7, the precision of stress wave detection was higher than that of drilling resistance detection. The precision of drilling resistance detection decreased slightly when the damaged proportion reached 1/5, but the precision increased with the increase of the damaged proportion. For elm, Figs. 10b and 10d show that the precision of stress wave detection went up or down. When the damaged proportion was 1/9 and 1/3, the precision of drilling resistance detection was higher than that of stress wave detection. When the damaged proportion was 1/7 and 1/5, the precision of stress detection was higher than that of drilling resistance detection. While the damaged proportion was 1/7, the precision of drilling resistance detection was the lowest. However, with the increase of the damaged, the precision of drilling resistance detection increased accordingly. Thus, when the damaged area is small, the precision of drilling resistance detection is higher than that of stress wave detection. With further increases in the damaged area, the precision curves of the two detection methods are close to each other.

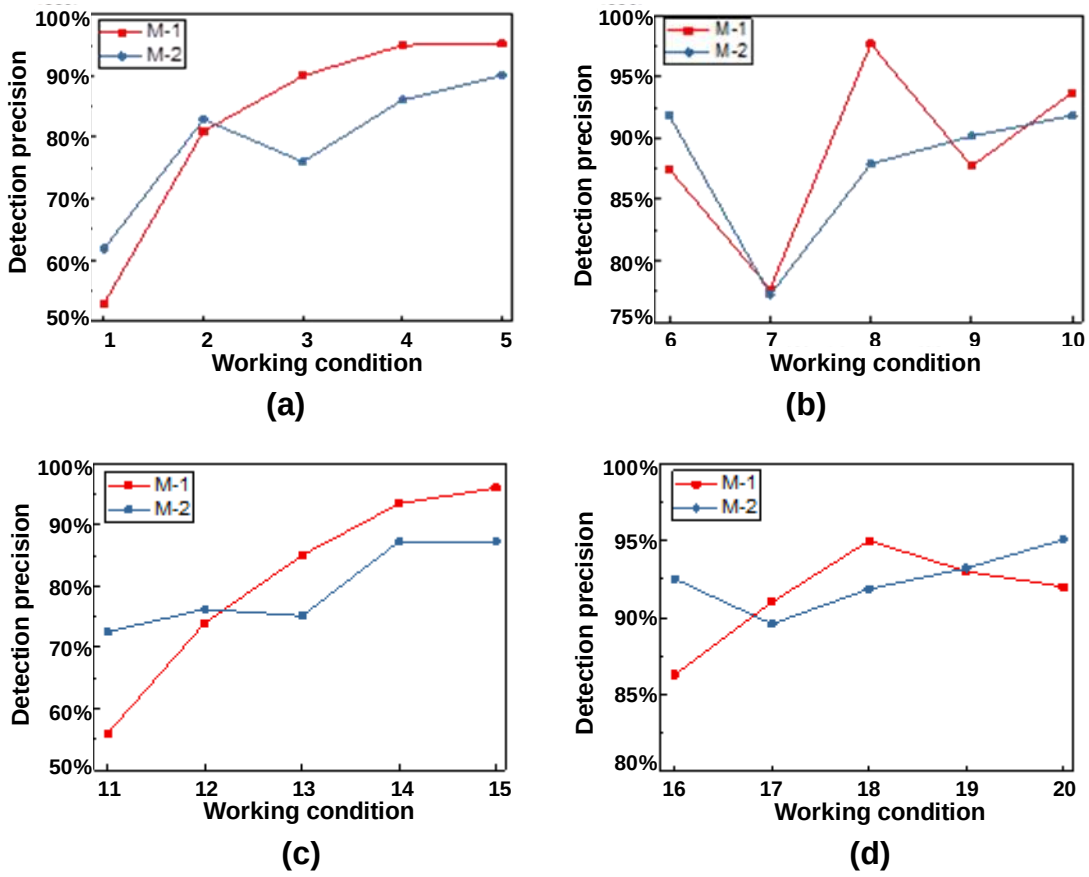

Fig. 10. Detection precision curves of (a) specimen1, (b) specimen2, (c) specimen3, (d) specimen4

To sum up, the combined use of stress wave detection and drilling resistance detection can screen the type, position and size of internal damage of timber components in ancient buildings, but the two detection results were quite different, and the detection precision was not high. In order to comprehensively utilize the information provided by the two detection methods, a combined forecasting model was established by assigning weighting coefficients to the different detection methods. It can unify and quantify the test results, so that the final forecasting results can make full use of the information obtained from each detection method, and effectively improve forecasting precision of the internal damage of timber components in ancient buildings.

Determine Combined Weight Coefficients

There are 20 working conditions which are based on two tree species, two types of damage and five damaged proportion mentioned in Table 1. Meanwhile, Table 2 shows the detection data based on 20 working conditions. According to the data in Table 2, information entropy, correlation coefficient and residual sum of squares of two detection methods are calculated by Eqs. 6, 7 and 8, respectively, as shown in Table 3.

Table 3. The Evaluation Criteria for the Errors of the Two Detection Methods

Method	Information entropy	Correlation coefficient	Residual sum of squares
M-1	0.8971	0.9891	12214.2355
M-2	0.9512	0.9958	18600.4148

Let the initial discourse domain U be {Information entropy, Correlation coefficient, Residual sum of squares},which can be expressed as$\{h_1,h_2,h_3\}$. As evaluation objects, two single detection methods are expressed as $A=\{S_1(t), S_2(t)\} = \{S_1, S_2\}$. The results of the evaluation criteria of detection error in Table 3 are taken as prior information, and the Delphi method is adopted to perform fuzzy evaluation on the evaluation objects to construct fuzzy soft mapping. The combined weight coefficients of the two detection methods is determined by using Bayesian formula combining prior information and expert weights.

The Delphi method was used to consult the ancient architecture experts and technical experts. When using stress wave detection and drilling resistance detection to detect internal defects of ancient wooden structures, let the two types of experts score the two detection methods according to this rating $H=\{0.1, 0.2,..., 1.0\}$ based on their experience. The results show that the weight interval of stress wave detection and drilling resistance detection given by the ancient architecture experts are 0.3~0.4 and 0.6~0.7, respectively. The weight interval of stress wave detection and drilling resistance detection given by the technical experts are 0.4 to 0.5 and 0.5 to 0.6, respectively. For the convenience of calculation, the average value was used. Based on input from the ancient architecture experts, the weight l_1 of stress wave detection and the weight l_2 of drilling resistance detection are 0.35 and 0.65, respectively. For the technical experts, the weight l_1 of stress wave detection and the weight l_2 of drilling resistance detection are 0.45 and 0.55, respectively. The prior information is normalized to construct the fuzzy soft mapping from A to U, as shown in Table 4.

Table 4. Fuzzy Soft Set

U	l_1	l_2
h_1	0.49	0.51
h_2	0.50	0.50
h_3	0.60	0.40
Expert 1	0.35	0.65
Expert 2	0.45	0.55

Note: Expert 1 represents the ancient architecture experts and Expert 2 represents the technical experts.

For expert 1, there are:

$$P(l_1|h_1)=\frac{P(h_1|l_1)P(l_1)}{\sum_{i=1}^{2}P(h_1|l_i)P(l_i)}=0.3410,\quad P(l_2|h_1)=\frac{P(h_1|l_2)P(l_2)}{\sum_{i=1}^{2}P(h_1|l_i)P(l_i)}=0.6590$$

$$P(l_1|h_2)=\frac{P(h_2|l_1)P(l_1)}{\sum_{i=1}^{2}P(h_2|l_i)P(l_i)}=0.3500,\quad P(l_2|h_2)=\frac{P(h_2|l_2)P(l_2)}{\sum_{i=1}^{2}P(h_2|l_i)P(l_i)}=0.6500$$

$$P(l_1|h_3)=\frac{P(h_3|l_1)P(l_1)}{\sum_{i=1}^{2}P(h_3|l_i)P(l_i)}=0.4468,\quad P(l_2|h_3)=\frac{P(h_3|l_2)P(l_2)}{\sum_{i=1}^{2}P(h_3|l_i)P(l_i)}=0.5532$$

Then,

$$l_{11}=\frac{1}{3}\left(P(l_1|h_1)+P(l_1|h_2)+P(l_1|h_3)\right)=0.3793,\quad l_{21}=\frac{1}{3}\left(P(l_2|h_2)+P(l_2|h_2)+P(l_2|h_3)\right)=0.6207$$

Similarly, for expert 2, there are:

$$l_{12}=\frac{1}{3}\left(P(l_1|h_1)+P(l_1|h_2)+P(l_1|h_3)\right)=0.4804,\quad l_{22}=\frac{1}{3}\left(P(l_2|h_2)+P(l_2|h_2)+P(l_2|h_3)\right)=0.5196$$

Finally, the corrected weights are:

$$l_1^*=\frac{l_{11}+l_{12}}{2}=0.43,\quad l_2^*=\frac{l_{21}+l_{22}}{2}=0.57$$

Table 5. Results of Different Combined Forecasting Models

Working conditions	Damaged proportion	Simulation type	Tree species	M-3			M-4		
				$\hat{S}_t$	$\hat{e}_t$	$\hat{p}_t$	$\hat{S}_t$	$\hat{e}_t$	$\hat{p}_t$
1	1/9	Hollow	Pine (Specimen 1)	82.02	1.26	89.12%	74.22	9.06	98.48%
2	1/7			105.38	1.69	94.45%	101.13	5.94	98.42%
3	1/5			135.87	14.03	86.90%	130.26	19.64	90.64%
4	1/3			235.40	14.44	92.14%	230.21	19.63	94.22%
5	1/2			361.35	13.41	94.80%	355.28	19.48	96.42%
6	1/9	Hollow	Elm (Specimen 2)	74.31	0.55	98.47%	72.63	1.13	99.25%
7	1/7			91.62	3.21	91.66%	86.92	7.91	96.62%
8	1/5			122.27	10.50	91.01%	120.84	11.93	92.09%
9	1/3			220.57	0.71	97.24%	215.18	6.10	99.68%
10	1/2			325.42	6.50	96.45%	320.15	11.77	98.04%
11	1/9	Insect attacks	Pine (Specimen 3)	110.59	3.50	95.41%	102.17	4.92	96.73%
12	1/7			134.45	3.24	92.17%	126.91	10.78	97.64%
13	1/5			177.87	14.89	87.89%	169.42	23.34	92.28%
14	1/3			307.02	14.25	93.44%	300.21	21.06	95.57%
15	1/2			438.51	43.40	90.03%	433.85	48.06	90.99%
16	1/9	Insect attacks	Elm (Specimen 4)	114.44	1.83	99.29%	111.82	0.79	98.38%
17	1/7			130.07	14.14	90.04%	129.85	14.36	90.20%
18	1/5			196.87	5.02	96.07%	193.95	7.94	97.51%
19	1/3			313.32	23.16	93.14%	313.40	23.08	93.12%
20	1/2			473.16	31.57	94.08%	474.85	29.88	93.74%
Mean value					11.07			14.84	

Note: $\hat{s}_t$, $\hat{e}_t$ and $\hat{p}_t$ are the forecasting value, the absolute error and the forecasting precision. M-3 represents the combined forecasting models based on fuzzy soft set and Bayesian method. M-4 represents the combined forecasting models based on entropy value.

According to Eq. 1, the combined forecasting model of internal damage in the timber components based on fuzzy soft set and Bayesian method can be written as follows:

$$\hat{S}_t=0.43S_{1t}+0.57S_{2t}\quad t=1,2,\cdots,20 \tag{11}$$

The data in Table 2 is substituted into Eq. 11 to calculate the combined forecasting value of internal damage in the timber components based on fuzzy soft set and Bayesian

method. For comparison, a combined forecasting model based on entropy value is introduced. The calculated results are listed in Table 5.

Analysis of Forecasting Results

In Table 5, the mean error of the combined forecasting models based on fuzzy soft set and Bayesian method is 11.07 cm^2, and the mean error of the combined forecasting models based on entropy value is 14.84 cm^2. Compared with stress wave detection, the mean error was reduced by 49.8% and 32.7%, respectively. Compared with drilling resistance detection, the mean error is reduced by 59.8% and 46.1%, respectively. Therefore, the combined forecasting models based on fuzzy soft set and Bayesian method had a lower forecasting error. Meanwhile, according to the evaluation principle of forecasting effect, *SSE*, *MSE*, *MAE*, *MAPE*, and *MSPE* were selected as evaluation indexes to reflect the effectiveness of two detection method and two combined forecasting models. The results are shown in Table 6. The formula of each evaluation index is as follows:

$$SSE=\sum_{t=1}^{n}(x_t-\hat{x}_t)^2,\quad MSE=\frac{1}{n}\sqrt{\sum_{t=1}^{n}(x_t-\hat{x}_t)^2},\ MAE=\frac{1}{n}\sum_{t=1}^{n}|x_t-\hat{x}_t|,\quad MAPE=\frac{1}{n}\sum_{t=1}^{n}|(x_t-\hat{x}_t)/x_t|,\ MSPE=\frac{1}{n}\sqrt{\sum_{t=1}^{n}[(x_t-\hat{x}_t)/x_t]^2}.$$

Table 6. Evaluation Indexes of the Forecasting Effect

Method	*SSE*	*MSE*	*MAE*	*MAPE*	*MSPE*
M-1	12214.2355	5.5259	22.0565	0.1399	0.0415
M-2	18600.4148	6.8192	27.5330	0.1517	0.0390
M-3	4845.8795*	3.4806*	11.0651*	0.0450*	0.0121*
M-4	6783.5006	4.1181	14.8404	0.0681	0.0170

Note: * represents the minimum value.

The results in Table 6 show that each effect index of the combined forecasting models based on fuzzy soft set and Bayesian method was better than that of the two single detection methods and the combined forecasting method based on entropy value. In order to fully express the overall forecasting effect of each method, the above five indexes were normalized to obtain the expression of comprehensive evaluation index *C*, which can be expressed as follows,

$$C_q=\frac{1}{n}\sum_{j=1}^{n}\min(E_j)/E_{qj} \quad (12)$$

where C_q is the comprehensive evaluation index of the *q-th* method, *q=1,2,3,4*; E_{qj} is the *j-th* index of the *q-th* method, *j=1,2,3,4,5*; *min* (E_j) is the minimum value among the *j-th* index of *m* methods. The higher C_q is, the better the corresponding method is. The comprehensive evaluation index C_q of each method is developed by bringing the five index values in Table 6 into Eq. 12.

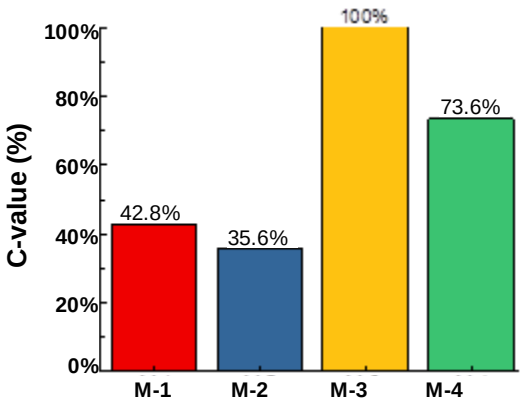

Fig. 11. Histogram of the index C_q for two detection methods and two forecasting methods

Figure 11 shows that the comprehensive evaluation index of each combined forecasting model was significantly higher than that of the two single detection methods, indicating that the combined forecasting model can improve the forecasting precision of the internal damage of the timber components. Furthermore, the *C* of the proposed method was higher than the others. The combined forecasting model based on fuzzy soft set and Bayesian method is the optimal model. It is a reliable and effective method for forecasting internal defect of ancient wooden components.

CONCLUSIONS

1. Most ancient wooden structures have been damaged for hundreds of years, so it is necessary to perform damage assessment on the ancient wooden components. The combined use of stress wave detection and drilling resistance detection can screen the type, position, and size of internal defect of ancient wooden components. The precision of the two detection methods is not high when the internal defects of the wood are small. As the proportion of the internal defects continues to increase, the detection precision of two detection methods has improved. However, the error of the two detection results is large and both exceed 10 cm^2, and the detection precision needs to be improved.
2. Based on two types of nondestructive testing data, this paper presents a combined forecasting model based on fuzzy soft set and Bayesian method to forecast the internal defect of wooden component in ancient buildings, which combines subjectivity and objectivity. Specifically speaking, the experts' evaluation fuzzy value is used to correct the prior information of nondestructive test through Bayesian formula to determine the combined weight coefficient. The corrected weight coefficient can accurately reflect the relative importance of the two detection methods in prediction evaluation. Comparative analysis results show that the forecasting average error of the model is reduced by 49.8% and 59.8% when compared with stress wave detection and drilling resistance detection. Meanwhile, based on five error indexes, the forecasting effect of this model is better than that of the combined prediction model based on entropy value, indicating that the combined forecasting model based on fuzzy soft sets and Bayesian method is more in line with practical application requirements and is a supplement to the method for predicting the internal defects of ancient wooden components.
3. Based on the above research foundation, the following research focuses on the

following points: (1) The precision of current stress wave detection technology for judging the range of defects in the wood and identifying the degree of defect decay is still low. The clarity of the two-dimensional image is not very high. This method needs to be improved. (2) Wood non-destructive testing should be expanded from two-dimensional space to three-dimensional space, and the three-dimensional imaging method of wood internal defects should be studied.

ACKNOWLEDGMENTS

This study was supported by the National Key R & D Program of China (Grant No. 2018YFD1100902-1), the National Natural Science Foundation of China (Grant No. 51678017), and Beijing Municipal Commission of Education-Municipal Natural Science Joint Foundation (Grant No. KZ202010005012).

REFERENCES CITED

Aggarwal, M. (2015). "A new family of induced OWA operators," *International Journal of Intelligent Systems* 30(2), 170-205. DOI: 10.1002/int.21693

An, Y., Yin, Y. F., Jiang, X. M., and Zhou, Y. C. (2008). "Inspection of decay distribution in wood column by stress wave and resistograph techniques," *Journal of Building Materials* 11(4), 457-463.

Broda, M., and Popescu, C. M. (2019). "Natural decay of archaeological oak wood versus artificial degradation processes-An FT-IR spectroscopy and X-ray diffraction study," *Spectrochimica Acta Part A* 209, 280-287. DOI: 10.1016/j.saa.2018.10.057

Calderoni, C., De Matteis, G., Giubileo, C., and Mazzolani, F. M. (2010). "Experimental correlations between destructive and non-destructive tests on ancient timber elements," *Engineering Structures* 32(2), 442-448.

Chang, L. H., Qian, W., and Dai, J. (2016a). "Combined predictive research on timber building internal defects," *Journal of Simulation Systems, Science and Technology* 17(25), 1473-8031.

Chang, L. H., Dai, J., and Qian, W. (2016b). "Nondestructive testing of internal defect of ancient architecture wood members based on Shapley value," *Journal of Beijing University of Technology* 42(6), 886-892.

Chang, L. H., Chang, X. H., Chang, H., Qian, W., Cheng, L. T., and Han, X. L. (2019). "Nondestructive testing on ancient wooden components based on Shapley value," *Advances in Materials Science and Engineering 2019*, Article ID 8039734. DOI: 10.1155/2019/8039734.

Chen, H. Y., and Hou, D. P. (2003). "Combination forecasting model based on forecasting effective measure with standard deviate," *Journal of Systems Engineering* 18(3), 203-210.

Chen, H. Y., and Sheng, Z. H. (2005). "A kind of new combination forecasting method based on induced ordered weighted geometric averaging (IOWGA) operator," *Journal of Industrial Engineering and Engineering Management* 19 (4), 36-39.

Chen, Y. P., and Guo, W. J. (2017). "Nondestructive evaluation and reliability analysis for determining the mechanical properties of old wood of ancient timber structure," *BioResources* 12(2), 2310-2325.

Choi, F. C., Li, J. C., Samali, B., and Crews, K. (2007). "Application of modal-based damage-detection method to locate and evaluate damage in timber beams," *Journal of Wood Science* 53 (5), 394-400. DOI: 10.1007/s10086-006-0881-5

Dackermann, U., Crews, K., Kasal, B., Li, J., Riggio, M., Rinn, F., and Tannert, T. (2014). "*In situ* assessment of structural timber using stress-wave measurements," *Materials and Structures* 47(5), 787-803. DOI: 10.1617/s11527-013-0095-4.

Dai, J., Chang, L. H., Qian, W., and Chang, H. (2017). "A study on the non-destructive method of testing internal and external defects of wooden components of historical buildings," *Architectural Journal* 2017(2), 7-10.

Dong, X. X., Chen, Y. X., Zhang, W. Y., and Zhang, F. (2018). "Combined forecasting approach for subsequent spare parts based on fuzzy soft set and Bayesian," *Journal of Nanjing University of Aeronautics and Astronautics* 50(5), 672-678.

Espinosa, L., Prieto, F., Brancheriau, L., and Lasaygues, P. (2019). "Effect of wood anisotropy in ultrasonic wave propagation: A ray-tracing approach," *Ultrasonic* 91, 242-251. DOI: 10.1016/j.ultras.2018.07.015

Franke, S., Franke, B., and Scharmacher, F. (2013). "Assessment of timber structures using the X-Ray technology," *Structural Health Assessment of Timber Structures Book Series: Advanced Materials Research* 778, 321-327. DOI: 10.4028/www.scientific.net/AMR.778.321

Gatto, D. A., Goncalves, M. R. F., Mattos, B. D., Calegari, L., and Stangerlin, D. M. (2012). "Evaluation of wood decay of floor of historic building using ultrasonic waves," *Cerne* 18(4), 651-656. DOI: 10.1590/S0104-77602012000400015

Gao, Z. W., Ma, D. H., Wang, W., Guo, X. D., and Ge, Q. Z. (2018). "Development and application of ancient timber buildings structural condition assessment model based on a fuzzy matter-element model that includes asymmetric proximity," *Mathematical Problems in Engineering*, Article Number: 7426915. DOI: 10.1155/2018/7426915

GB/T 50005 (2017). "Standard for design of timber structures," Standardization Administration of China, Beijing, China.

GB/T 50329 (2012). "Standard for test methods of timber structures," Standardization Administration of China, Beijing, China.

Ge, X. W., Wang, L. H., Sun, T. Y., Liu, Z. X., and Bao, Z. Y. (2014). "Quantitative detection of salix matsudana inner decay based on stress wave and resistograph techniques," *China Forestry Science and Technology*, 28(5), 87-91.

Huang, R. F., Wu, Y. M., Li, H., and Liu, X. Y. (2010). "Quantitative analysis of decaying detected by Pilodyn in wood of ancient architecture," *Scientia Silvae Sinicae* 46(10), 114-118.

Huang, R. D., Zhang, H. B., Yang, Z. H., Zhou, Y., and Zhang, P. (2015). "Research and application of multi-criteria combination forecast model," *Journal of Central South University of Science and Technology* 46(5), 1778-1785.

Isik, F., and Li, B. L. (2003). "Rapid assessment of wood density of live trees using the resistograph for selection in tree improvement programs," *Canadian Journal of Forest Research* 33(12), 2426-2435. DOI: 10.1139/X03-176

Kasal, B., and Anthony, R. W. (2004). "Advances in in-situ evaluation of timber structures," *Progress in Structural Engineering and Materials* 6 (2), 94-103.

Kim, Y. J., and Park, S. J. (2017). "Tectonic traditions in ancient Chinese architecture, and their development," *Journal of Asian Architecture and Building Engineering* 16(1), 31-38. DOI: 10.3130/jaabe.16.31

Kovkov, D. V., Kolbanov, V. M., and Molodtsov, D. A. (2007). "Soft sets theory-based

optimization," *International Journal of Computer and Systems Sciences* 46(6), 872-880. DOI: 10.1134/S1064230707060032

Li, X., Dai, J., Qian, W., and Chang, L. H. (2015). "Prediction of internal defect area in wooden components by stress wave velocity analysis," *BioResources* 10(3), 4167-4177.

Lianxiao and Morimoto, T. (2019). "Spatial analysis of social vulnerability to floods based on the MOVE framework and information entropy method: Case study of Katsushika Ward, Tokyo," *Sustainability* 11(2), 36-39. DOI: 10.3390/su11020529

Molodtsov, D. (1999). "Softset theory-First results," *Computers and Mathematics with Applications* 37(4), 19-31.

Nowak, T. P., Jasienko, J., and Hamrol-Bielecka, K. (2016). "*In situ* assessment of structural timber using the resistance drilling method-Evaluation of usefulness," *Construction and Building Materials* 102(1), 403-415. DOI: 10.1016/j.conbuildmat.2015.11.004

Ouis, D., and Zerizer, A. (2006). "Modeling rot in wood by replacement of wood with sand: An experimental study," *Journal of Wood Science* 52(3), 208-212. DOI: 10.1007/s10086-005-0762-3

Pease, B. J., Scheffler, G. A., and Janssen, H. (2012). "Monitoring moisture movements in building materials using X-ray attenuation: Influence of beam-hardening of polychromatic X-ray photon beams," *Construction and Building Materials* 36, 419-429. DOI: 10.1016/j.conbuildmat.2012.04.126

Qin, S. J., and Yang, N. (2016). "Investigation of damage condition of Chinese ancient timber buildings," *Fundamental Research in Structural Engineering: Retrospective and Prospective* 1 and 2, 1390-1395.

Riggio, M., Sandak, J., and Franke, S. (2015). "Application of imaging techniques for detection of defects, damage and decay in timber structures on-site," *Construction and Building Materials* 101(2), 1241-1252. DOI: 10.1016/j.conbuildmat.2015.06.065

Rust, S., and Göcke, L. (2000). "A new tomographic device for the non-destructive testing of standing tree," in *Proceedings of the 12th International Symposium on Nondestructive Testing of Wood*, Sep, University of Western Hungary, Sopron.

Shannon, C. E. (1948). "A mathematical theory of communication," *Bell System Technical Journal* 27(3), 379-423 (623–656).

Sun, T. Y. (2014). "Application of fuzzy soft set and Bayesian formula to index weight determination," *Journal of Chongqing Technology and Business University (Natural Science Edition)* 31(5), 34-38.

Vossing, K. J., and Niederleithinger, E. (2018). "Nondestructive assessment and imaging methods for internal inspection of timber," *Holzforschung* 72(6), 467-476. DOI: 10.1515/hf-2017-0122

Vossing, K. J., Gaal, M., and Niederleithinger, E. (2018). "Air-coupled ferroelectret ultrasonic transducers for nondestructive testing of wood-based materials," *Wood Science and Technology* 52(6), 1527-1538. DOI: 10.1007/s00226-018-1052-8

Wang, X. P., and Allison, R. B. (2008). "Decay detection in red oak trees using a combination of visual inspection, acoustic testing, and resistance microdrilling," *Arboriculture & Urban Forestry* 34(1), 1-4.

Wang, Z. Y., Ma, D. H., Qian, W., Wang, W., Guo, X. D., Xu, Q. F., Huan, J. H., and Gao, Z. W. (2019). "Detection and prediction of internal damage in the ancient timber structure based on optimal combined model," *Advances in Civil Engineering* 2019, Article ID 7108262. DOI: 10.1155/2019/7108262

Wu, S. J., Xu, J. M., Li, G. Y., Risto, V., Lu, Z. H., Li, B. Q., and Wang, W. (2010). "Use of the pilodyn for assessing wood properties in standing trees of *Eucalyptus* clones," *Journal of Forestry Research* 21 (1), 68-72. DOI: 10.1007/s11676-010-0011-5

Yue, F., Su, Z. P., Lu, Y., and Zhang, G. F. (2013). "Comprehensive evaluation of software quality based on fuzzy soft sets," *Systems Engineering & Electronics* 35(7), 1460-1466.

Zhou, S. Q., and Wang, J. Q. (2009). "Combined forecasting approach based on multi-criteria optimization," *Systems Engineering & Electronics* 31(7), 1651-1654.

Zhu, G. Y., and Yan, H. S. (2004). "A combination forecasting method based on model evaluation and selection from forecasting-model-base," *Control and Decision* 19(7), 726-731.

Article submitted: October 21, 2019; Peer review completed: December 8, 2019; Revised version received and accepted: December 17, 2019; Published: December 21, 2019.
DOI: 10.15376/biores.15.1.1134-1153